Behavior of a sustainable composite floor system with deconstructable clamping connectors

Lizhong Wang
Department of Civil and Environmental Engineering, Northeastern University
Boston, MA, USA
wang.l@husky.neu.edu

Mark D. Webster
Simpson Gumpertz & Heger Inc.
Waltham, MA, USA
MDWebster@sgh.com

Jerome F.Hajjar
Department of Civil and Environmental Engineering, Northeastern University
Boston, MA, USA
JF.Hajjar@northeastern.edu

ABSTRACT

This paper presents the behavior of a sustainable composite steel/concrete floor system under gravity and seismic loading. In this system, precast concrete planks are attached to steel beams using deconstructable clamping connectors, enabling reuse of the structural components and reducing the energy consumption related to material fabrication and waste disposal. The results of several composite beam tests are presented along with the companion pushout tests. In the pushout tests, both monotonic and cyclic load-slip curves were established for the clamping connectors. Full-scale composite beams were then designed and tested to investigate the flexural behavior of the system under gravity loading.

INTRODUCTION

In 2012, buildings are responsible for approximately 47.6% of the energy consumption and 44.6% of the CO2 emission in the U.S. (Energy Information Administration 2012; Architecture 2030, 2013). To preserve the natural environment, the building industry has to be transformed from the major contributor to the solution to climate changes and global warming. In addition to exploiting renewable energy, reduction of energy consumption and emission of greenhouse gases is most effectively achieved by implementing sustainable design strategies, such as selecting materials and products with lower embodied energy, utilizing energy efficient operating systems, adopting deconstructable structural systems to maximize material reuse, etc. Great progress has been made to optimize material and energy use, for example, replacing cement in concrete with fly ash (Bilodeau et al. 2000), designing green roofs to reduce the solar radiation reaching the structures below (Castleton et al. 2010), etc. However, limited research is focused on new structural systems

to facilitate design for deconstruction, particularly for composite construction (Lam et al. 2013; Lee et al. 2013).

As the most ubiquitous type of structural steel framing for commercial and institutional buildings, steel-concrete composite floor systems make efficient use of the two materials, with concrete being subjected to compression and steel resisting tension. However, the integration of steel beams and concrete slabs via shear studs inhibits the separation of the two materials, making impossible the deconstruction of the composite flooring systems and reuse of the structural components. Steel beams and shear studs can be recycled after being extracted from demolition debris, while concrete slabs are crushed for fill or making aggregates for new concrete. Conventional composite floor systems are therefore not the best choice for reducing the long-term environmental impacts of building materials.

In this paper, a sustainable composite floor system is presented. Deconstructable clamping connectors are utilized to attach the precast concrete planks to the steel beams, and the planks are connected in-plane with post-tensioned rods. To investigate the behavior of the floor system under gravity and seismic loading, both pushout tests and composite beam tests were conducted. In the pushout tests, both monotonic and cyclic load-slip curves were established for the clamping connectors. Full-scale beam tests were then performed to study the strength, stiffness, and ductility of the composite beam specimens.

DECONSTRUCTABLE COMPOSITE FLOOR SYSTEM

The deconstructable composite prototype is illustrated in Figure 1; this concept was first introduced in Webster et al. (2007).This system is designed to maintain the benefits of steel-concrete composite construction, such as enhanced flexural strength and stiffness, reduced steel beam size and weight, and ease of construction, and to enable sustainable design of composite floor systems in steel building structures, components disassembly and reuse of the structural components.

In this system, high-strength T-bolts, which are inserted into the cast-in channels embedded in precast concrete planks, are pretensioned to firmly clamp the top flanges of the steel beams with the underside of the concrete planks. Composite action is thus achieved by utilizing the friction generated at the steel-concrete interface and the steel-clamp interface. In addition to deconstructability, the proposed system also offers adaptability and flexibility in that no predrilled holes are required, and the embedded channels allow for beams with different flange widths.

Grouting precast concrete panels and placing a cast-in-place topping are common in conventional precast concrete construction, but they may impede the deconstruction of the system and are thus not recommended. Therefore, load transfer under gravity loading is achieved with tongue and groove joints that also facilitate alignment during construction. Shown in Figure 2, unbonded threaded rods are post-tensioned to clamp adjacent concrete planks, and the resulting friction resists plank joint sliding under shear and plank joint opening under flexure during earthquakes. The planks are staggered to assist diaphragm load transfer in the perpendicular direction and to enhance reuse flexibility. After the end-of-life of the structural system, the precast concrete planks and steel beams can be easily disassembled and reconfigured in future projects by loosening the bolts and rods.

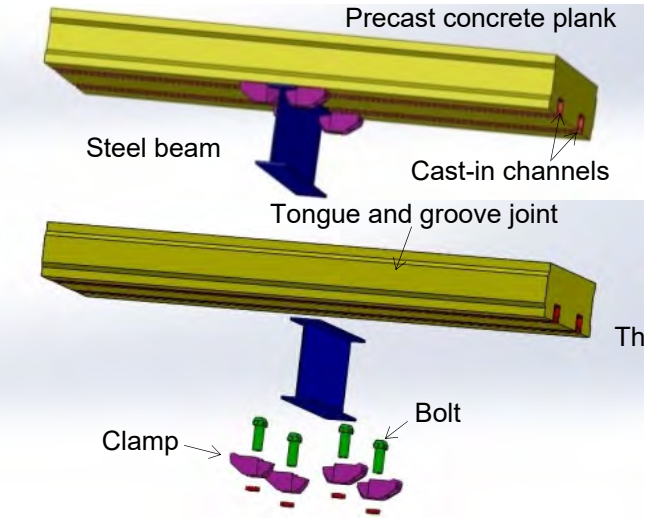

Fig. 1 - Deconstructable composite beam prototype

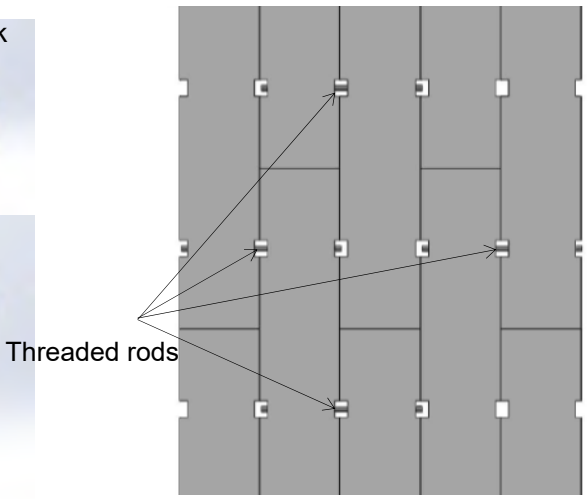

Fig. 2 - Precast concrete plank connections

PUSHOUT TESTS

Pushout tests were conducted under both monotonic and cyclic loading to establish the behavior of the clamping connections for both gravity applications and for use as fasteners to accomplish load transfer between diaphragms and lateral load-resisting systems in seismic applications.

Pretension tests

For the T-bolt connections, as the nut is turned, both the T-bolt heads and the channel lips deform. Consequently, the nut rotation calibrated for regular bolted connections, which is given in Table 8.2 in RCSC Specification (2009), does not apply to the pretensioning of the T-bolts. Pretension tests were thus performed to decide the number of turns of nut. The pretension test configuration is given in Figure 3. Three bolts were snug-tightened to restrain the movement of the beam, whereas the tested bolt was first snug-tightened and then torqued until fracture.

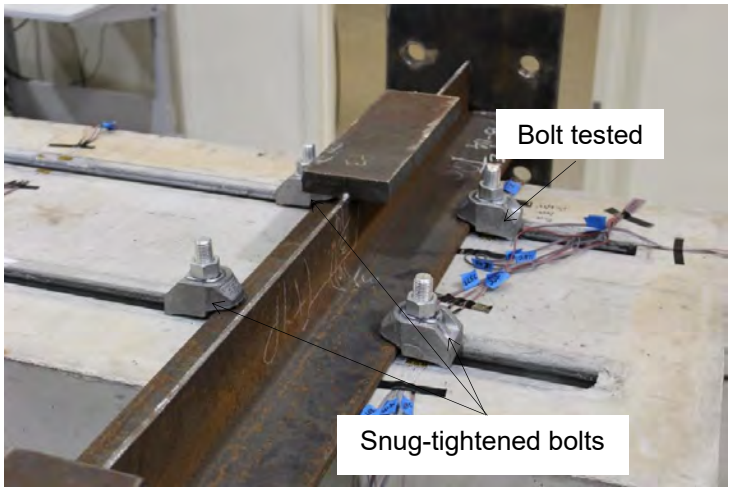

Fig. 3 – Pretension test setup

M24 bolts

M20 bolts

Fig. 4 – Fractured bolts

As shown in Figure 4, three M24 and M20 bolts were tested, and the axial strain variation was tracked for each bolt throughout the test using uniaxial strain gages attached on the bolt shank.

The bolt axial stress was then converted from the strain measurements utilizing the stress-strain curves obtained from tensile testing of round coupons machined from the bolts. Because bolt yielding is clearly shown in the plots in Figure 5, 2.0 turns and 1.5 turns after a snug-tight condition are recommended for pretensioning the M24 and M20 bolts, respectively.

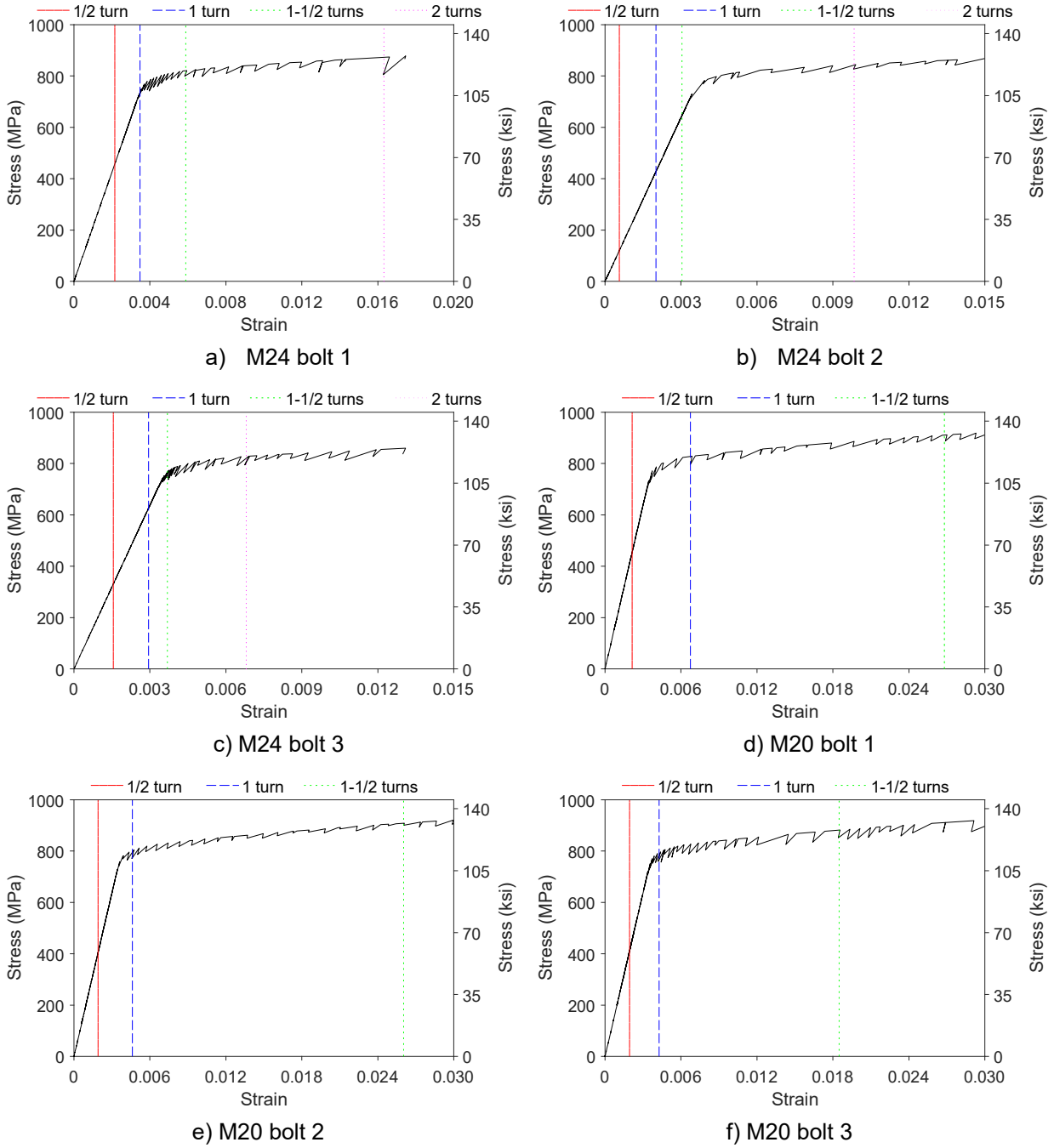

Fig. 5 – Bolt axial stress and strain variation in pretension tests

Pushout tests

As shown in Figure 6, each pushout specimen consisted of a 4 ft. x 2 ft. x 6 in. (1219 mm x 610 mm x 152 mm) concrete plank connected with a WT5x30 or WT4x15.5 section using either M24

or M20 clamps. The specimen was mounted upside down to view the motion of the clamps and steel beam. The pushout test matrix is given in Table 1. The light reinforcement configuration was designed only for gravity loading, while additional supplementary reinforcement was placed around the channel anchors to prevent anchor-related concrete failure modes. Since the flanges of the WT4x15.5 sections were very thin, testing of the WT4x15.5 sections with the M24 clamps required shims placed between the clamps and the steel beam flanges. The specimen naming convention is explained using Specimen 3-M24-T4-RH-S, with M describing monotonic loading, 24 describing M24 bolts, T4 describing two-channel specimens, RH describing heavy reinforcement configuration, and S describing shims. More details about the test configuration and test matrix can be found in Wang et al. (2015).

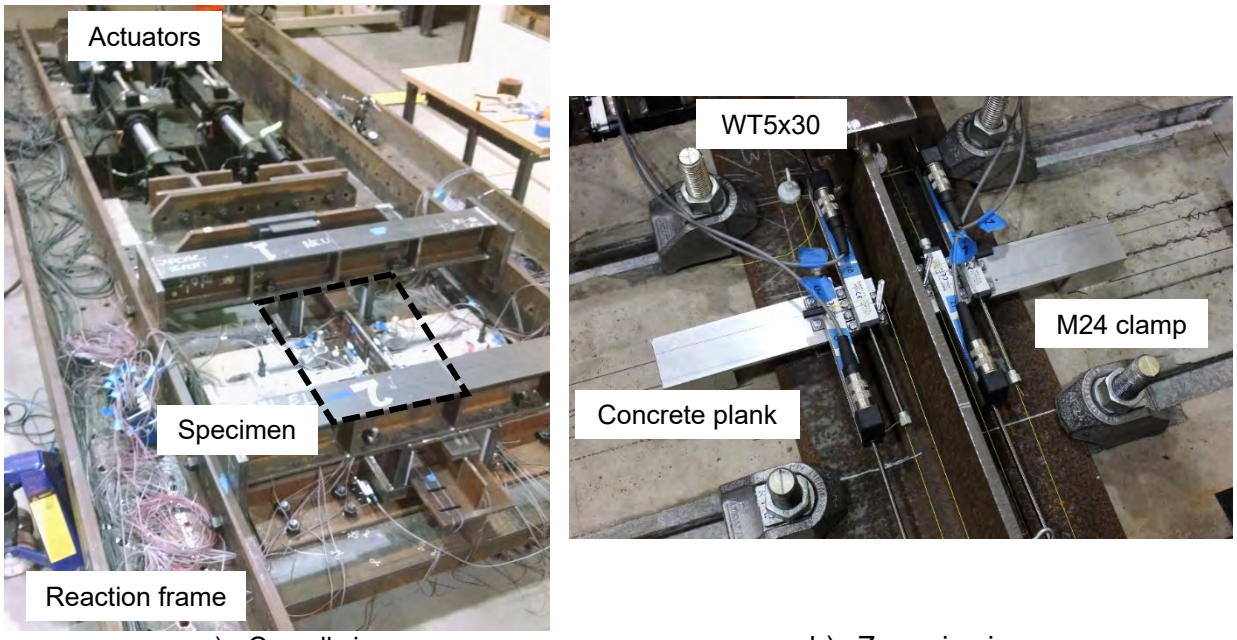

a) Overall view b) Zoom-in view

Fig. 6 – Typical pushout test specimen

Table 1 - Pushout test matrix

Series	Specimen	Test parameters				Number of turns
		Bolt diameter	Number of T bolts	Reinforcement configuration	Shim	
M	2-M24-T4-RH	M24	4	Heavy	No	3 turns
M	3-M24-T4-RH-S	M24	4	Heavy	Yes	3 turns
M	4-M24-T6-RH	M24	6	Heavy	No	2 turns
M	5-M20-T4-RH	M20	4	Heavy	No	1.5 turns
C	6-C24-T4-RH	M24	4	Heavy	No	2 turns
C	7-C24-T4-RL	M24	4	Light	No	2 turns
C	8-C24-T4-RH-S	M24	4	Heavy	Yes	2 turns
C	9-C24-T6-RH	M24	6	Heavy	No	2 turns
C	10-C20-T4-RH	M20	4	Heavy	No	1.5 turns

The pushout test results are illustrated in Figure 7 and Figure 8. The load-slip curves of Specimens 2-M24-T4-RH and 4-M24-T6-RH exhibit ductile behavior and excellent slip capacity. Provided the limit state is fracture in the stud shank, the peak shear strength of a 19 mm (3/4 in.) diameter shear stud embedded in a solid concrete slab is 95.6 kN (21.5 kips), close to 98.3 kN (22.1 kips) which is the average shear strength of an M24 clamp. Both specimens retained almost 80% of their peak strengths at a slip of 127 mm (5 in.). In contrast, according to the statistical analysis conducted by Oehlers and Coughlan (1986), the mean ultimate slip of shear studs is 7.4 mm (0.29 in.). Initially, three complete turns of nut were applied to the bolts in the first two tests (Tests 2 and 3) before it was determined in subsequent pushout tests to use 2.0 turns of nut for the M24 clamps, as discussed above. The head of one of these bolts fractured in Test 3-M24-T4-RH-S because of the excessive rotation, as is demonstrated by the sharp strength drop at a slip around 25.4 mm (1 in.). Shortly after the fracture, load oscillation occurred, which could be attributed to a stick-slip mechanism exaggerated by the shims. The stick-slip behavior was also confirmed in prior research by Grigorian et al. (1994) on the cyclic behavior of clamped bolted connections with steel-steel sliding surfaces. Compared to the M24 clamps, the post-peak strength of the M20 clamps degraded more quickly because the M20 clamps were smaller and they were prone to rotate when significant displacements occurred along the steel beam, as shown in Figure 9. This was due to the channel lips (which were the same size for all tests) not being adequately large to support the M20 clamps as fully as the M24 clamps were supported, or due to the contact of the clamp teeth with the steel flange having too small an area compared to the M24 clamp. Consequently, the bolt pretension decreased as the clamps rotated. It might be advised that the M20 clamping connections be redesigned to delay rotation, e.g., a design where the embedded channel restrains the rotation of the clamp using an interlocking connection, in which case it is anticipated that the behavior of the clamps will be comparable to the M24 clamps in this work.

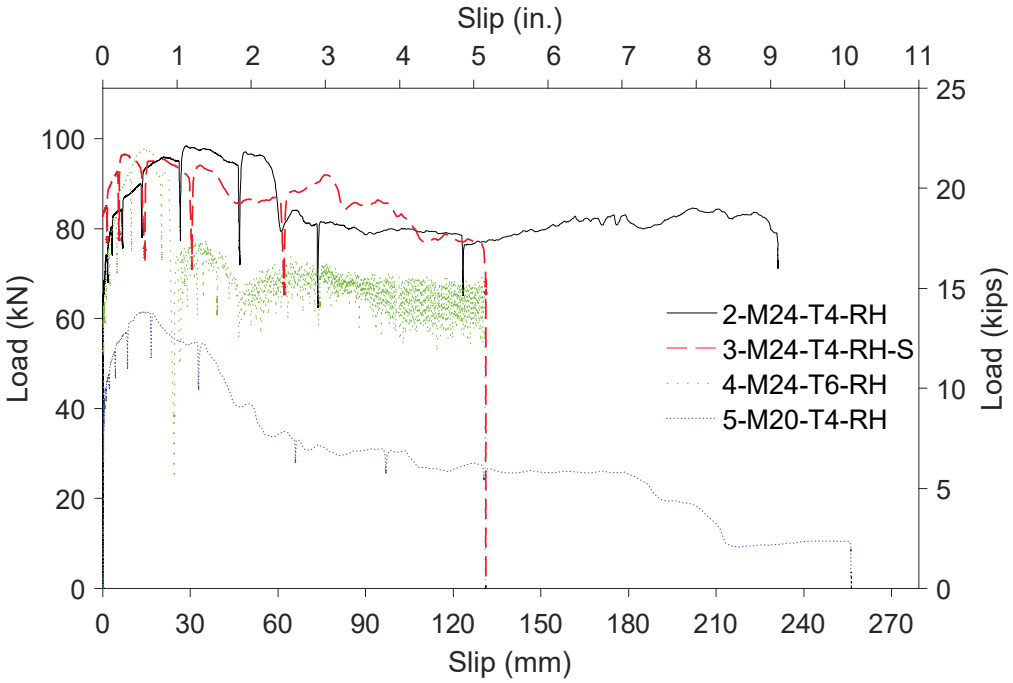

Fig. 7 – Load-slip curves of monotonic specimens (per connector)

Similar to the strength reduction seen in shear studs under cyclic loading (Pallarés et al 2009), the cyclic load-slip curves of the clamping connectors also exhibit decreasing shear strength as the cyclic behavior continues. In the clamping system, the abrasion between the concrete plank and the steel beam and between the clamp and the steel beam smoothed the contact surfaces and damaged the clamp teeth and the steel flanges, lowering the frictional coefficients and releasing the bolt pretension, as shown in Figure 10. This strength reduction can be accounted for in design, thus enabling the clamping connectors to be designed reliably to connect composite diaphragms and lateral load-resisting systems due to the excellent energy dissipation. The lightly reinforced concrete plank did not display any anchor-related concrete failure modes, and the comparison in Figure 8 also indicates that the light reinforcement configuration had negligible effects on the strength of Specimen 7-C24-T4-RL. Also, as seen when comparing monotonic specimens 2-M24-T4-RH and 3-M24-T4-RH-S, and cyclic specimens 6-C24-T4-RH and 8-C24-T4-RH-S, adding a shim between the clamp and steel flange produced oscillations due to stick-slip behavior and may not be recommended for design.

All the tests were terminated when the stroke of the linear potentiometers was reached or when all the clamps detached from the steel beam. No other specific limit states were observed.

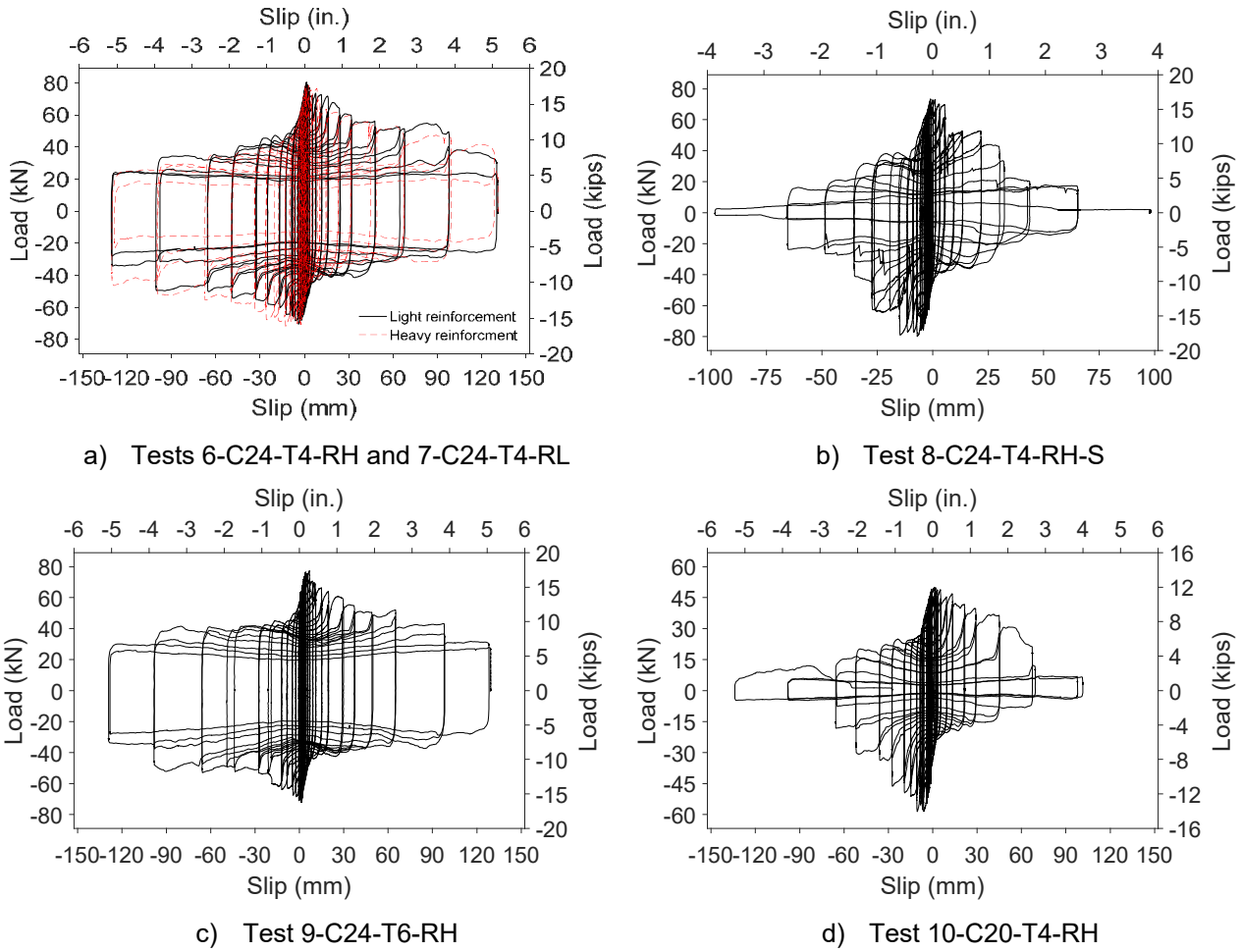

a) Tests 6-C24-T4-RH and 7-C24-T4-RL

b) Test 8-C24-T4-RH-S

c) Test 9-C24-T6-RH

d) Test 10-C20-T4-RH

Fig. 8 – Load-slip curves of cyclic specimens (per connector)

Fig. 9 – Large rotation of M20 clamp

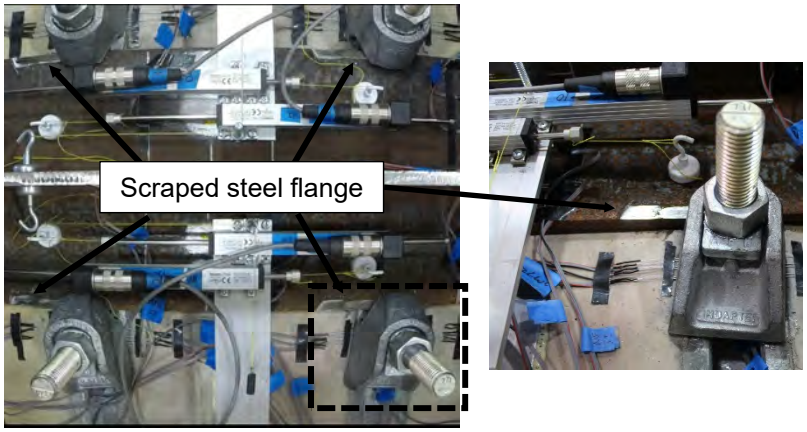

Fig. 10 – Damage of the steel flange in Test 6 at 1.28 in. (32.5 mm) slip

COMPOSITE BEAM TESTS

After completing the pushout tests, four full-scale composite beams were designed and tested. As shown in Figure 11, each beam specimen consisted of a 30-foot (9144 mm) long beam attached with fifteen 2-ft.-wide (609.6 mm) planks using clamping connectors. The actuator loads were spread using spreader beams at four points along the length (six-point bending) to mimic a secondary beam under approximately uniform loading. A pin support and a roller support were placed at the ends of the beams to permit horizontal movement as well as end rotation. Braces were utilized to prevent lateral deformation of the system due to accidental eccentricity existing in the test setup and load application. To simplify specimen construction, tongue and groove joints at the plank edges shown in Figure 1 were eliminated. Grade A36 5/8 in. (16 mm) diameter fully threaded rods were utilized to connect adjacent concrete planks to resist in-plane diaphragm forces. One full turn of nut from the snug-tight position was determined for pretensioning the rods after performing calibration tests in which rods passing through two planks were torqued until fracture. The concrete planks were 8 ft. (2438 mm) wide, which is sufficient to avoid any premature concrete failure in narrow slabs (Grant et al. 1977). The composite beam test matrix is given in Table 2. The naming convention of the specimens is explained using Test 2-M24-1C-RL, with M24 describing M24 bolts, 1C describing one channel embedded in each concrete plank, RL describing light reinforcement pattern. The heavy reinforcement pattern contained not only bars required to resist negative bending of the planks under concentrated loads but also supplementary rebar placed around channel anchors.

Fig. 11 – Composite beam test setup

Table 2 – Composite beam test matrix

Composite beam #	Bolt size	Beam size	Reinforcement configuration	# of clamps	Degree of composite action
1-M24-2C-RH	M24	W14x38	Heavy	56	82.7%
2-M24-1C-RL	M24	W14x38	Light	30	45.1%
3-M20-3C-RL	M20	W14x26	Light	90	137.8%
4-M20-1C-RL	M20	W14x26	Light	30	43.8%

The specimens were loaded to 40% of their expected flexural strength and then reloaded three times. Two more cycles were then undertaken, with one cycle at 60% and the other one at 80% of the estimated flexural strength. These cycles were intended to mimic serviceability conditions. After completing the loading/unloading cycles, the beams were then loaded until the deflections were excessive, surpassing *L*/25, where *L* is the beam span. All the beams were shored during construction, and the load-deflection curves plotted in Figure 12 are shifted from the origins to account for the bending moment and deflection under the self-weight of the composite beam and loading structures. All the beams demonstrated ductile behavior. Major events are identified on the curves, including slip of the clamps, yielding of the steel beam, concrete crushing, and first bang heard during the test. Slip is identified when the maximum relative movement between the steel beam and the concrete planks is larger than 0.02 in. Bangs were heard when abrupt slips occurred between the steel beam and the concrete planks. All the tests were terminated because of excessive deflection.

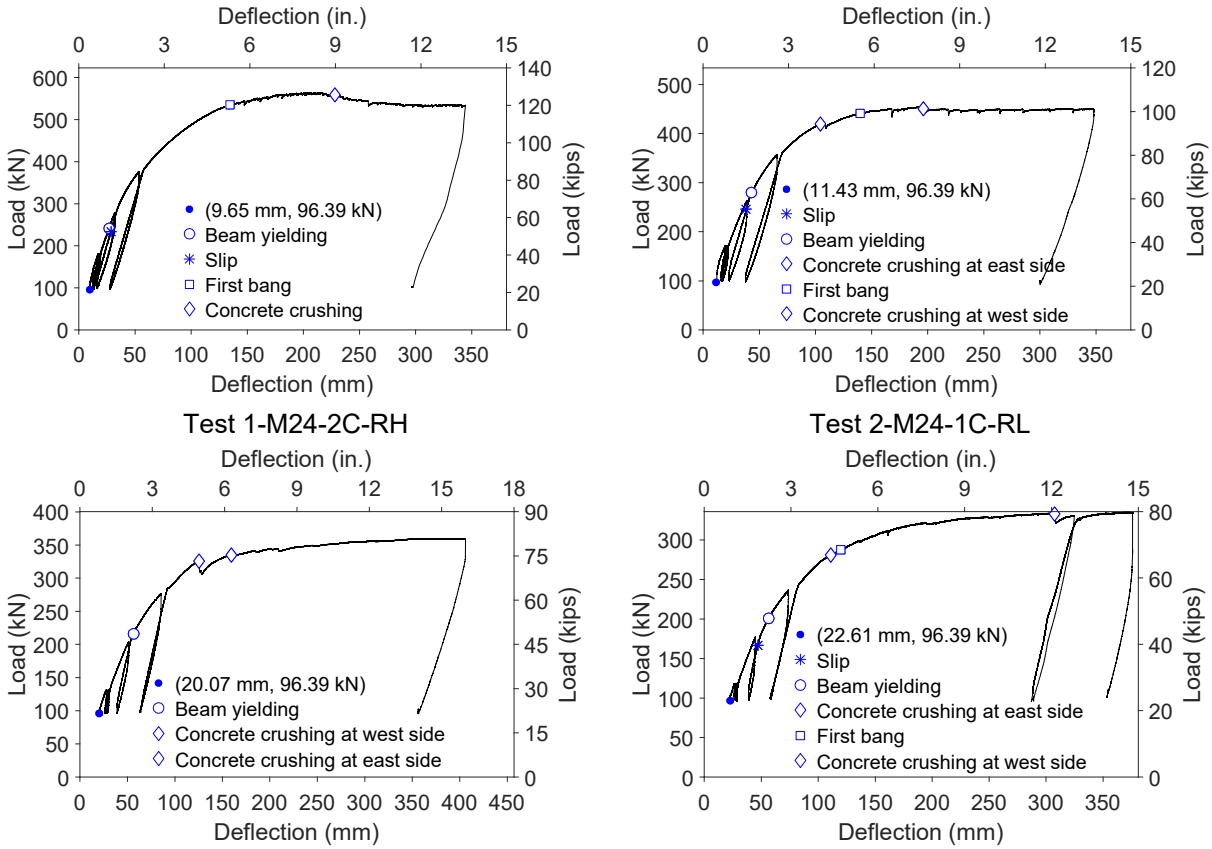

Fig. 12 – Load-deflection curves of composite beam specimens

The key results are summarized in Table 3 for all the specimens. For the specimens using the same steel section, the stiffness increases as the percentage of composite action of the beam increases. The stiffness calculated using a lower bound moment of inertia [I_{LB} from AISC (2016)] is below the tested stiffness of the deconstructable composite beam specimens and establishes that I_{LB} remains an appropriate lower bound estimate for these composite beams. The reason could be the different mechanisms of achieving composite action for the two types of shear connectors, with clamping connectors relying on the friction between the structural components and shear studs bearing against concrete slabs. The ultimate flexural strengths of the beams are also predicted using AISC design equations (AISC 2016), and the tested strengths are close to the predictions. It is seen that the degree of shear connection is proportional to the degree of composite action, with the maximum and minimum amount of slip occurring in beams with the smallest and largest degree of composite action, respectively. In the composite beam tests, the maximum slip demand on the clamping connectors was much smaller than the clamp slip demand during the pushout tests. After completing the tests, the composite beams were disassembled and a deconstructed steel beam is shown in Figure 14. The beam is intact except for the impressions on the top flange under the clamp teeth. In typical applications where a beam would not be subjected to ultimate loads, it is anticipated the steel beam would be in its elastic state when deconstructed.

Table 3 – Composite beam test results

Specimen #	Stiffness			Moment			Max slip mm (in.)	
	Test	AISC	Test/AISC	Test	AISC	Test/AISC		
	kN/mm (kips/in.)			kN-m (ft-kips)			West end	East end
1-M24-2C-RH	9.24 (52.8)	8.67 (49.5)	1.07	777 (571)	767 (566)	1.01	5.94 (0.234)	6.43 (0.253)
2-M24-1C-RL	7.76 (44.3)	6.81 (38.9)	1.14	634 (469)	632 (466)	1.00	8.18 (0.322)	6.45 (0.254)
3-M20-3C-RL	6.46 (36.9)	5.99 (34.2)	1.08	494 (364)	510 (376)	0.97	0.46 (0.018)	0.23 (0.009)
4-M20-1C-RL	6.08 (34.7)	4.43 (25.3)	1.37	476 (351)	400 (295)	1.19	8.79 (0.346)	8.08 (0.318)

Fig. 13 – Concrete crushing between planks

Fig. 14 – Deconstructed steel beam

CONCLUSIONS

A new deconstructable composite floor system is proposed to promote sustainable design of composite floor systems within bolted steel building construction through comprehensive reuse of all key structural components.

Based on the pretension tests, 2.0 turns and 1.5 turns after a snug-tight condition were recommended for pretensioning the M24 and M20 bolts in the deconstructable composite floor system. Under monotonic loading, the pushout specimens using M24 clamps were ductile, with almost 80% of their peak strengths retained at a slip of 127 mm (5 in.). In contrast, the post-peak strength of the M20 clamps declined more quickly because the clamps were prone to rotate as the beam moved. Nonetheless, the slip at which the curve started to descend was much larger than the slip demand on shear connectors in composite beams. If the rotation were restrained or an interlocking component design were developed, the M20 clamps would behave similarly as the M24 clamps. Because of the abrasion between the steel flange and the concrete plank and between the steel flange and the clamps, the strengths of the cyclic pushout specimens were lower than the strengths of the corresponding monotonic specimens; this reduction should be accounted for in design. Adding a shim between the clamp and steel flange produced oscillations due to stick-slip behavior and may not be recommended for design. The hysteresis load-slip loops demonstrate the potential of the clamping connectors to transfer in-plane diaphragm forces.

Four composite beams of different levels of composite action were designed and deflected to about L/25. Although some localized concrete crushing occurred along the top edges of the precast planks at large deflections, all the beams behaved in a ductile manner with little or no strength degradation. Compared to the stiffness calculated using a lower bound moment of inertia, the actual stiffness of the deconstructable composite beam specimens was slightly larger. The tested flexural strengths of the beams were close to those predicted by the AISC (2016) design equations. The specimens were readily deconstructed after the testing was completed.

The channel, T-bolt, and clamp are commercially available components. The components are not designed to work together in the proposed configuration, which resulted in certain behavior limitations that could be addressed by the development of modified components tailored to this particular application.

ACKNOWLEDGMENTS

This material is based upon work supported by the National Science Foundation under Grant No. CMMI-1200820 and Grant No. IIS-1328816, the American Institute of Steel Construction, Northeastern University, and Simpson Gumpertz and Heger. In-kind support is provided by Benevento Companies, Capone Iron Corporation, Fastenal, Halfen, Lehigh Cement Company, Lindapter, Meadow Burke, S&F Concrete, and Souza Concrete. This support is gratefully acknowledged. The authors would like to thank Kyle Coleman, Michael McNeil, Kurt Braun, Corinne Bowers, Edward Myers, Majed Alnaji, Madeline Augustine, Ian Carver, Morgan Foster, Michael Bangert-Drowns, Kara Peterman, Angelina Jay, Justin Kordas, David Padilla-Llano, and Yujie Yan for their assistance with the experiments. Any opinions, findings, and conclusions expressed in this material are those of the authors and do not necessarily reflect the views of the National Science Foundation or other sponsors.

REFERENCES

AISC (2016). *Specification for Structural Steel Buildings*, American Institute of Steel Construction, Chicago, Illinois.

Architecture 2030 (2013). Available at: http://architecture2030.org/buildings_problem_why/ (accessed April 2017).

Bilodeau, A. and Malhotra, V. M. (2000). “High-Volume Fly Ash System: Concrete Solution for Sustainable Development,” *ACI Materials Journal*, Vol. 97, No. 1, pp. 41-50.

Castleton, H. F., Stovin, V., Beck, S. B., and Davison, J. B. (2010). “Green roofs; building energy savings and the potential for retrofit”. *Energy and buildings*, Vol. 42, No. 10, pp. 1582-1591.

Energy Information Administration (2012), *Annual Energy Review*, U.S. Energy Information Administration, Washingtong, D.C.

Grant, J. A., Fisher, J. W., and Slutter, R. G. (1977). “Composite beams with formed steel deck,” *Engineering Journal*, Vol. 14, No.1, pp. 24-43.

Grigorian, C. E., and Popov, E. P. (1994), "Energy Dissipation with Slotted Bolted Connections,” Report UCB/EERC-94/02, Earthquake Engineering Research Center, College of Engineering, University of California at Berkeley, Berkeley, California.

Lam, D., Dai, X., and Saveri, E. (2013), "Behavior of Demountable Shear Connectors in Steel-Concrete Composite Beams," *Composite Construction in Steel and Concrete VII*, American Society of Civil Engineers, July 2013, Queensland, Australia, pp. 618-631.

Lee, S. S. M., and Bradford, M. A. (2013), “Sustainable composite beam behavior with deconstructable bolted shear connectors,” *Composite Construction in Steel and Concrete VII*, American Society of Civil Engineers, July 2013, Queensland, Australia, pp. 445-455.

Oehlers, D. J., and Coughlan, C. G. (1986). "The shear stiffness of stud shear connections in composite beams," *Journal of Constructional Steel Research*, Vol. 6, No. 4, pp. 273-284.

Pallarés, L. and Hajjar, J. F. (2009). “Headed Steel Stud Anchors in Composite Structures: Part I. Shear,” Report No. NSEL-013, Newmark Structural Laboratory Report Series (ISSN 1940-9826), Department of Civil and Environmental Engineering, University of Illinois at Urbana-Champaign, Urbana, Illinois, April.

RCSC (2009). *Specification for Structural Joints Using High-Strength Bolts*, Research Council on Structural Connections, Chicago, Illinois.

Wang, L., Webster, M. D., and Hajjar, J. F. (2015). “Behavior of Deconstructable Steel-Concrete Shear Connections in Composite Beams,” Proceedings of the 2015 SEI Structures Congress, Portland, Oregon, April 23-25, 2015, ASCE, Reston, Virginia.

Webster, M., Kestner, D., Parker, J., Johnson, M. (2007) “Deconstructable and Reusable Composite Slab,” Winners in the Building Category: Component – Professional Unbuilt, Lifecycle Building Challenge http://www.lifecyclebuilding.org/2007.php